

Supersolid and charge density-wave states from anisotropic interaction in an optical lattice

Y.-H. Chan, Y.-J. Han, and L.-M. Duan

Department of Physics and MCTP, University of Michigan, Ann Arbor, Michigan 48109

(Dated: May 10, 2010)

We show anisotropy of the dipole interaction between magnetic atoms or polar molecules can stabilize new quantum phases in an optical lattice. Using a well controlled numerical method based on the tensor network algorithm, we calculate phase diagram of the resultant effective Hamiltonian in a two-dimensional square lattice — an anisotropic Hubbard model of hard-core bosons with attractive interaction in one direction and repulsive interaction in the other direction. Besides the conventional superfluid and the Mott insulator states, we find the striped and the checkerboard charge density wave states and the supersolid phase that interconnect the superfluid and the striped solid states. The transition to the supersolid phase has a mechanism different from the case of the soft-core Bose Hubbard model.

PACS numbers: 37.10.Jk, 67.85.Jk

The remarkable experimental realization of ultracold dipolar molecules [1] and ultracold atoms with large magnetic moments [2] open up the possibilities of probing novel phases of matter that are induced by strong dipole-dipole interaction. Among these possibilities, a particularly interesting one is the supersolid phase, where superfluidity coexists with a charge density wave order [3]. In a square lattice, the supersolid state has been predicted to exist for soft-core bosons if the off-site interaction gets comparable with the on-site interaction [4]. For ultracold atoms, it is challenging to experimentally realize this condition, as even with the long-range dipole interaction, the interaction strength still falls off quickly with distance. In an optical lattice, the on-site interaction is typically much larger than the off-site interaction, and if one increases the interaction strength (or equivalently reduce the atomic tunnelling rate), one enters the hard-core boson region where each site can only have one or zero atom due to the interaction blockade. For hard core bosons in the conventional square lattice, with only the neighboring interaction, the supersolid state can not be stabilized [5], and one has to rely on more unusual interaction configuration (such as a Hamiltonian with strong next-nearest-neighbor interaction [6]) or lattice geometry (such as a triangular lattice [7]) to stabilize such a phase. A recent interesting study based on quantum Monte Carlo simulation has shown, however, with true long-range interaction that falls off with distance by the cubic form, the supersolid state can be stabilized for hard-core bosons in a square lattice [8]. As the supersolid state can not be stabilized by the neighboring interaction alone, the small energy scale associated with the long-range tail of the dipole interaction clearly plays an important role in determining the stability region of the supersolid state in that case.

The dipole interaction has two characteristic features: first, it is relatively long-range; and second, the interaction form is anisotropic in space. Ref. [8] has shown that

the long range tail of the dipole interaction, even under an isotropic interaction form, can lead to stabilization of the supersolid state. Complementary to this research, in this paper we show that by tuning the anisotropy of the dipole interaction, we can stabilize a supersolid state even if we neglect the small long range tail of the dipole interaction. The supersolid state here is of a different type compared with the case studied in [8] as we have a stripe instead of a checkerboard density-wave order. The anisotropy of the dipole interaction has been analyzed recently under a mean-field treatment of the Hamiltonian for the soft-core bosons [9]. The mean-field approximation, however, typically overestimates the stability region of the supersolid state. For instance, it would predict a checkerboard supersolid state for hard-core bosons in a square lattice, which is actually unstable to quantum fluctuation [5]. In this paper, we use a well-controlled numerical method based on the recently developed tensor network algorithm to calculate the phase diagram of hard-core bosons in a two-dimensional square lattice. We construct quantitative phase diagrams under different interaction parameters, and analyze the properties of the transition from the striped solid phase to the supersolid state. The transition has a mechanism different from the case of the soft-core Bose Hubbard model [4].

We consider a system where bosonic dipolar molecules (or magnetic atoms) are confined to a two-dimensional (2D) optical lattice, denoted here as $x - z$ plane. Initially the orientation of the external field is controlled such that all the dipoles point to the y axis. The strength of the dipole-dipole interaction depends on θ_{ij} , the angle between the orientation of the dipole moments and their relative positions, as $(1 - 3\cos^2\theta_{ij})$. Thus we have isotropic repulsive interaction at the beginning when the direction of the dipole is perpendicular to the $x - z$ plane ($\theta_{ij} = \pi/2$). Due to the strong repulsive dipole interaction, we assume the system is in the hard-core boson region with each site occupied by less than one molecule.

Then we adiabatically tune the direction of the external field towards the $x - z$ plane to change the anisotropy of the dipole interaction. Depending on the angle θ_{ij} , the interaction may get attractive along one direction and repulsive along the other direction. With the attractive interaction, one may expect that more than one bosons can occupy the same site for the ground state. There is also concern about stability of the system under the attractive interaction. However, as we start with a configuration with no double occupation, the energy shift Δ from the strong on-site interaction forbids two bosons jumping to the same site due to the energy conservation. This is true independent of the sign of Δ , as long as its magnitude $|\Delta|$ is much larger than the atomic tunnelling rate. In addition, the possible instability of the double occupation (or multiple occupation) states will further suppress the probability of double occupation due to the dissipation-induced blockade mechanism (the quantum Zeno effect) [10]. As a net result, when we tune the interaction to the attractive region, the system remains stable in an optical lattice and still stays in the hard-core boson region with negligible double occupation. As the dipole interaction falls off with distance pretty quickly by the cubic law, in this paper we keep the off-site interaction only to the order of nearest neighbors. So the focus of investigation here is on new properties induced by the anisotropy of the dipole interaction, not by its small long-range tail. The Hamiltonian of this system can then be described as hard-core bosons on a 2D square lattice with anisotropic nearest neighbor interactions

$$H = - \sum_{\langle i,j \rangle} t(b_i^\dagger b_j + h.c.) - \sum_i \mu b_i^\dagger b_i + \sum_j (V_x n_j n_{j \pm \hat{e}_x} + V_z n_j n_{j \pm \hat{e}_z}) \quad (1)$$

where b_i^\dagger is the boson creation operator at site i , $n_i = b_i^\dagger b_i$, t is the atomic tunnelling rate over the nearest neighbors $\langle i, j \rangle$, μ is the chemical potential, and V_x (V_z) are respectively the nearest neighbor interaction rates in the x (z)-direction.

The hard core bosons live in a truncated Hilbert space spanned by only two states $|0\rangle$ and $|1\rangle$, representing respectively zero or one boson on a site. The commutation relation of the hard-core boson operators is thus modified to $[b_i, b_i^\dagger] = |0\rangle\langle 0| - |1\rangle\langle 1| = 1 - 2n_i$. With the well known mapping of the hard-core boson operators to the Pauli operators through $b_i^\dagger \rightarrow \sigma_i^+$ and $2n_i - 1 \rightarrow \sigma_i^z$, the hard core boson Hamiltonian in Eq. (1) is equivalent to the following anisotropic XXZ model

$$H = - \sum_{\langle i,j \rangle} J_{xy}(\sigma_i^x \sigma_j^x + \sigma_i^y \sigma_j^y) + V_x/4 \sum_j \sigma_j^z \sigma_{j+\hat{e}_x}^z + V_z/4 \sum_j \sigma_j^z \sigma_{j+\hat{e}_z}^z - h \sum_j \sigma_j^z \quad (2)$$

where $J_{xy} = 2t$ and $h = \mu/2 - 2$. The chemical potential μ acts as an effective magnetic field along the z direction in the resulting XXZ model. With different signs of V_x and V_z , one can have ferromagnetic coupling in one direction and anti-ferromagnetic coupling in the other direction.

We numerically study the phase diagram of this Hamiltonian by using the iPEPS algorithm [11]. The iPEPS algorithm is an extension of the well-known DMRG (density-matrix renormalization group) method to 2D quantum systems. It is a variational approach based on the tensor network states (or called the PEPS states) that appropriately capture the entanglement structure of the 2D quantum systems. The iPEPS algorithm has been tested to work reliably for a number of 2D many-body models [12]. We have tested our numerical codes for implementation of the iPEPS algorithms by comparing our calculation results with the known results for several many-body models, including the 2D Ising model with a transverse field and the XXZ model. In general, the results are in quantitative agreement with the previous quantum Monte Carlo simulation and the PEPS calculation from other groups, and the phase transition points can be determined with a pretty good precision (the error is typically about or less than a percent level). So we expect that with the same algorithm, we can reliably determine the phase diagram of the anisotropic XXZ model shown in Eq. (2). In our simulation, we use a bond dimension up to $D = 4$ or 5 for the variational tensor network states and a large enough cutoff dimension χ (typically of the order of D^2) in contraction of the tensor network states to ensure converge of the ground state energy.

A typical phase diagram of the Hamiltonian (1) is shown in Fig 1. We take $t = 1$ as the energy unit and scan over different μ and V_x with a fixed V_z . To identify different phases, we calculate the superfluid order parameter $\langle b_i \rangle$ and the boson occupation number $\langle n_i \rangle$ at different sites as functions of μ and V_x . These curves show different characteristic behaviors and we can use them to identify different phases.

Figure 1 shows the phase diagram when V_z is fixed at $-t$ and V_x is scanned over the positive region. First, we note in Fig. 1 there is a large region of the charge density wave state at exactly half filling, which has a stripe order. This phase can be easily understood: with negative V_z and positive V_x , at half filling the particles arrange themselves into stripes along the z direction to maximize the neighboring interaction along the z direction and simultaneously minimize the repulsive coupling along the x direction. The most interesting feature from Fig. 1 is that the stripe phase is always surrounded by a finite region of the supersolid state that interconnects the superfluid phase and the charge density wave state. The supersolid state here is characterized by coexisting of the superfluid order and the stripe charge density wave or-

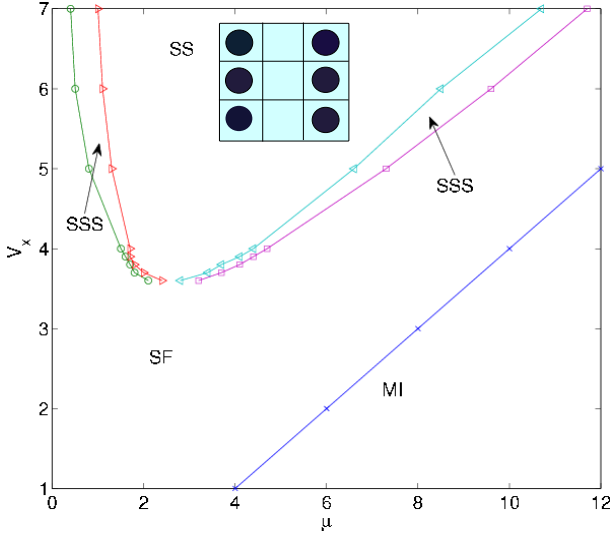


FIG. 1: (Color Online) Zero-temperature Phase diagram of the extended Bose Hubbard model with anisotropic interaction shown in Eq. (1) at $V_z = -t$. As one varies the chemical potential μ and the interaction rate V_x (both in the unit of the hopping rate t), four different phases are observed, including the superfluid (SF) phase, the striped solid (SS) phase, the striped supersolid (SSS) phase, and the Mott insulator (MI) state. The inset shows schematically the particle filling pattern in the striped solid phase.

der. The optimal condition to get the supersolid state is to have V_z negative and comparable with the tunnelling rate t in magnitude.

To better understand the transition to the supersolid state, in Fig. 2 we show the evolution of the superfluid order parameter $\langle b_i \rangle$ and the particle occupation number $\langle n_i \rangle$ at two alternating sites i and $i + 1$ along the x direction as we scan the chemical potential μ . Starting from a striped solid state at half filling, we enter the supersolid phase with either particle or hole doping. When we add particles to the half filled lattice (with increase of the chemical potential), while the occupation of the initially empty sites increases, the average occupation of the initially filled sites (which form the stripes) continuously decreases. This shows that with particle doping, some particles need to move from the initially filled stripes to the empty sites to build up the superfluid order. As the superfluid order increase, the charge density wave order continuously decreases and eventually vanishes, and one enters the normal superfluid phase. The transitions from the striped solid phase to the supersolid and from the supersolid to the superfluid phase are both of the second order characterized by kinks in the first-order derivatives of the ground state energy. We have a similar picture of the supersolid transition at the side of the hole doping where we exchange particles with holes. This picture of the supersolid transition is different from the mechanism of the supersolid state for soft core bosons in a lattice

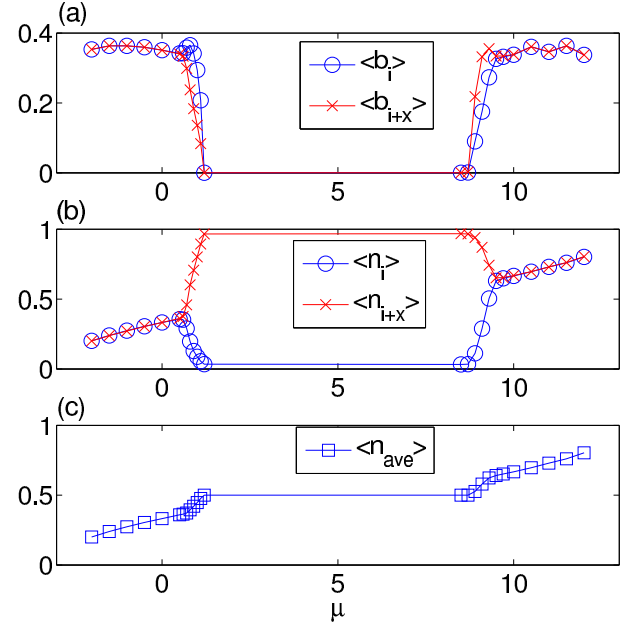


FIG. 2: (Color Online) The order parameters and the filling numbers as functions of the chemical potential. (a): The superfluid order parameters $\langle b_i \rangle$ and $\langle b_{i+\hat{x}} \rangle$ at two alternating sites along the x -direction (the direction perpendicular to the stripes). (b): The filling number (the particle per site) $\langle n_i \rangle$ and $\langle n_{i+\hat{x}} \rangle$ at two neighboring sites along the x -direction. (c): The average number per site $\langle n_{ave} \rangle = (\langle n_i \rangle + \langle n_{i+\hat{x}} \rangle)/2$. The interaction parameters in these figures are taken as $V_x = 6t$ $V_z = -t$. The kinks in Figs. (a)-(c) mark two continuous phase transitions from the superfluid to the supersolid and then to the striped solid phase.

with large neighboring interaction [4]. In the latter case, starting with a checkerboard lattice at half filling, the supersolid phase only appears with particles doping (no supersolid with hole doping), and as one add particles, these added particles continuously go to the already filled sites to maintain the checkerboard order. As one increase the chemical potential, the occupation of the initially filled sites continuously increase for the checkerboard supersolid phase (instead of decrease for the striped supersolid phase discussed above).

In the supersolid state, we can look at both the superfluid and the density-density correlations, and these correlations are shown in Fig. 3. The superfluid density is not homogeneous in space. In Fig. 3a, we can see that along the x direction (perpendicular to the stripe direction), the superfluid correlation shows the zigzag pattern, but it is extended to the long range. Along the stripe (z) direction, the superfluid correlation is monotonic and approaches a constant nonzero value. This constant value, however, is different for the particle-dominated and the hole-dominated stripes. When the filling number is less than one half (hole doping to the stripe solid state), the superfluid density is larger in the particle-dominated stripes. The reverse is true for the supersolid state with

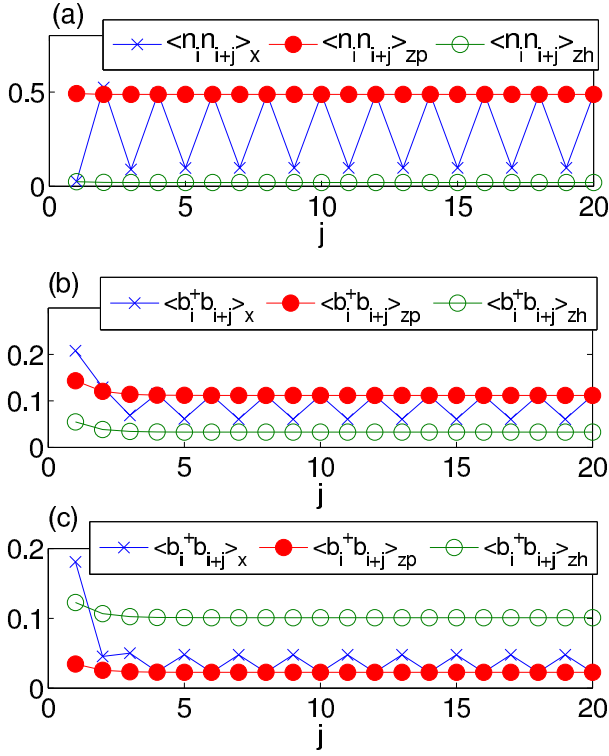


FIG. 3: (Color Online) The density-density and the superfluid correlations in the supersolid phase. Figs. (a) and (b) are for the supersolid phase with hole doping to the striped solid state at half filling (with the parameters $V_z = -1$, $V_x = 6$, and $\mu = 0.9$ in the unit of the hopping rate t). The density-density (a) and the superfluid (b) correlations are shown along the x and the z directions, distinguished by the subindices x (along the x -direction), zh (along the hole dominated stripe in the z direction), and zp (along the particle dominated stripe in the z direction). Fig. (c) represents the corresponding superfluid correlations for the supersolid phase with particle doping to the stripe solid phase (with the parameters $V_z = -1$, $V_x = 6$, and $\mu = 9.1$). One can see that with the hole doping, the superfluid correlation is stronger along the particle dominated stripe; the reverse is true for the case of the particle doping.

the filling number larger than one half (see Fig. 3c). The density-density correlation is shown in Fig. (3a), which shows a long-range zigzag pattern along the x direction, but with constant correlation along the stripes (z direction) as the density distribution along the stripes is homogeneous.

In the phase diagram shown in Fig.1, one can see that both the stripe solid state and the supersolid phase disappear when the repulsive interaction along the x direction becomes weak. As a result, there is only the conventional superfluid to the Mott insulator transition, and the strip phase at half filling becomes unstable. This instability can be intuitively understood as follows: assume we have a strip phase, and we move one particle from the filled stripe to the empty stripe to form a particle-hole excitation. The cost in the interaction energy is given

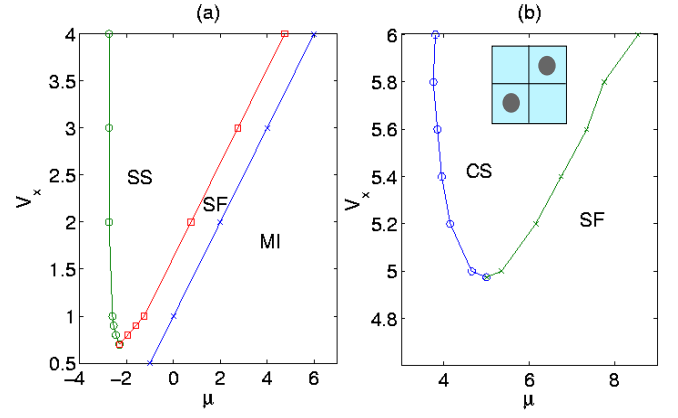


FIG. 4: (Color Online) Phase diagram of the Hamiltonian (1) with interaction rate $V_z = -3$ for Fig. (a) and $V_z = 0$ for Fig. (b) (in the unit of the hopping rate t). There is no supersolid phase in either of these two cases. At half filling, one has a striped solid phase for Fig. (a) and a checkerboard solid phase for Fig. (b). The insert in Fig. (b) shows schematically the particle filling pattern in the checkerboard phase.

by $2V_x - 2V_z$. At the same time, as the particle and the hole can freely move, the kinetic energy is lowered by an amount $8t$. The net energy cost is positive when $2V_x - 2V_z - 8t > 0$, and in this case the stripe phase is stable. Otherwise, the freely-moving particle-hole pairs will be continuously generated to form a superfluid phase and the stripe phase loses its stability. With this simple estimate, we see that for $V_z = -t$, the stripe phase becomes unstable when $V_x < 3t$, which roughly agrees with the accurate calculation of the boundary of the phase diagram shown in Fig. 1. This simple estimate also applies to the cases with different V_z . For instance, in the phase diagrams shown in Fig.4 for different values of V_z , the point where the charge wave density (solid) phase loses its stability at half filling can still be roughly estimated by $V_x < V_z + 4t$.

As we increase or decrease the interaction V_z away from its optimal value around $-t$, the region of the supersolid phase gets smaller. With a stronger attractive interaction (larger $|V_z|$), the stripe solid phase gets larger in the phase diagram, however, the intermediate supersolid phase, which requires a careful balance of the interaction energy and the kinetic energy to enable coexistence of both the superfluid and the charge-density wave orders, cannot be stabilized in this case. We have a direct transition from the superfluid phase to the striped solid phase. The evolution of the corresponding order parameter is shown in Fig. 5, which indicates that this transition is of the first order. With a weaker V_z , the supersolid region also gets smaller. As we turn off V_z or scan V_z to the positive region, the charge-density wave state at half filling has a checkerboard order instead of a stripe order. For the transition from the superfluid phase to the checkerboard solid phase, we do not find any su-

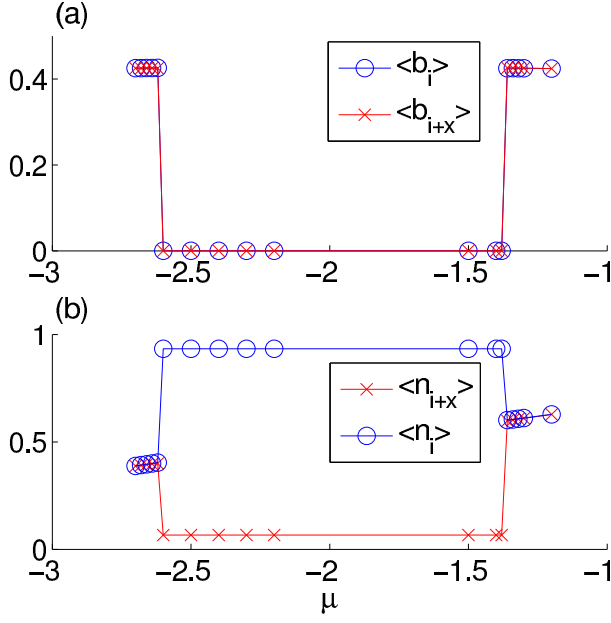


FIG. 5: (Color Online) The superfluid (Fig. a) and the charge density wave (Fig. b) order parameters are shown as functions of the chemical potential μ for the phase diagram shown in Fig. (4a) with the interaction parameters $V_x = 1$ $V_z = -3$ (in the unit of the hopping rate t). Notations have the same meaning as in Fig. 2. The transition from the superfluid to the striped solid phase is clearly of the first order.

persolid state in the intermediate region. This finding is consistent with the result from quantum Monte Carlo simulation of the XXZ model in a square lattice (which corresponds to a particular case of the Hamiltonian (2) with isotropic coupling $V_z = V_x > 0$), which shows that the supersolid phase predicted by the mean-field theory is unstable to quantum fluctuation [5]. The evolution of the order parameters as functions of the chemical potential follow very similar curves as those shown in Fig. 5, and the transition from the superfluid to the checkerboard phase is also of the first-order.

In summary, we have shown that anisotropy of the dipole interaction between magnetic atoms or polar molecules can stabilize new quantum phases in an optical lattice. By tuning the orientation of the external field, we argue that the system can be described as a extended hard-core Bose-Hubbard model with attractive interac-

tion along one direction and repulsive interaction along the other direction in a two-dimensional square lattice. Starting from appropriate initial states, the insatiability and the atom clustering associated with the attractive interaction can be overcome in an optical lattice through the blockade effect induced by both the atomic interaction and the collision loss. Using a well controlled numerical method based on the tensor network algorithm, we calculate the phase diagram of the extended hard-core Bose-Hubbard model with anisotropic interaction, and find a significant region of the supersolid phase that interconnects the striped solid phase at half filling and the conventional superfluid state. The properties of the supersolid phase and the corresponding phase transitions are discussed and characterized through calculation of various kinds of correlation functions.

We thank Guin-Dar Lin for helpful discussions. This work is supported by the DARPA OLE Program under ARO Award W911NF0710576, the AFOSR MURI program, the IARPA, and the ARO MURI program.

-
- [1] K.-K. Ni et al., Science 322, 231 (2008); K.-K. Ni et al., Nature 464, 1324 (2010).
 - [2] T. Koch et al., Nat. Phys. 4, 218 (2008); M. Lu, S.-H. Youn, and B. Lev, Phys. Rev. Lett. 104, 063001 (2010).
 - [3] E. Kim and M.H.W. Chan, Nature 427, 225 (2004).
 - [4] P. Sengupta et al., Phys. Rev. Lett. 94, 207202 (2005).
 - [5] G.G. Batrouni and R.T. Scalettar, Phys. Rev. Lett. 84, 1599 (2000).
 - [6] F. Hebert et al., Phys. Rev. B 65, 014513 (2002).
 - [7] S. Wessel and M. Troyer, Phys. Rev. Lett. 95, 127205 (2005).
 - [8] B. Capogrosso-Sansone et al., Phys. Rev. Lett. 104, 125301 (2010).
 - [9] I. Danshita and C.A.R. Sa de Melo, Phys. Rev. Lett. 103, 225301 (2009).
 - [10] N. Syassen, D. M. Bauer et al., Science 320, 1329 (2008); J. J. Garcia-Ripoll et al., New J. Phys. 11, 013053 (2009); Y.-J. Han et al., Phys. Rev. Lett. 103, 070404 (2009).
 - [11] J. Jordan et al., Phys. Rev. Lett. 101, 250602 (2008).
 - [12] J. Jordan, R. Orus and G. Vidal, Phys. Rev. B 79, 174515 (2009); B. Bauer, G. Vidal, and M. Troyer, arXiv:0905.4880, J. Stat. Mech. P09006 (2009).